Low Mode Number Stability of a Quadrupole Tandem Mirror

M.W. Phillips and J.D. Callen

July 1983

UWFDM-530

FUSION TECHNOLOGY INSTITUTE

UNIVERSITY OF WISCONSIN

MADISON WISCONSIN

Low Mode Number Stability of a Quadrupole Tandem Mirror

M.W. Phillips and J.D. Callen

Fusion Technology Institute
University of Wisconsin
1500 Engineering Drive
Madison, WI 53706

http://fti.neep.wisc.edu

July 1983

UWFDM-530

LOW MODE NUMBER STABILITY OF A QUADRUPOLE TANDEM MIRROR

M.W. Phillips† and J.D. Callen

Fusion Engineering Program
Nuclear Engineering Department
University of Wisconsin-Madison
Madison, Wisconsin 53706

July 1983

UWFDM-530

† Present address: Grumman Aerospace Corporation, 105 College Road East, Princeton, NJ 08540.

Low Mode Number Stability of a Quadrupole Tandem Mirror

M.W. Phillips[a] and J.D. Callen

Nuclear Engineering Department
University of Wisconsin-Madison
Madison, Wisconsin 53706

Abstract

We study the low mode number macroscopic stability of plasmas in the Phaedrus tandem mirror. Our stability analysis includes finite Larmor radius effects and takes into account the nonaxisymmetric nature of the equilibrium. A variational principle is formulated which is solved for the normal modes of the system by a Rayleigh-Ritz method. Despite the full 3-D representation of the modes and nonaxisymmetry of the equilibrium it is found that for values of $\rho_i/R_p > 0.05$ the most unstable modes are to a large extent composed of a single poloidal Fourier (m) component. For Phaedrus the most unstable mode is an m = 1 rigid displacement.

[a] Present address: Grumman Aerospace Corporation, 105 College Road East, Princeton, NJ 08540.

I. Introduction

Most present day tandem mirror experiments rely on quadrupole end plugs to provide average minimum-B stability. The quadrupole end plugs make the overall geometry of a tandem mirror nonaxisymmetric. In this paper we address the effect this nonaxisymmetric nature of a tandem mirror has on the stability of low poloidal mode number MHD modes. Experimental evidence indicates that the MHD stability of tandem mirrors is determined by low mode number perturbations. Low mode number modes are usually global in nature and thus the nonaxisymmetric nature of the equilibrium becomes more important. Also, in a nonaxisymmetric geometry poloidal and radial mode components can couple and thus a full 3-D representation of the mode is needed.

For large m-number modes the nonaxisymmetry of a quadrupole tandem mirror is not a problem. Utilizing an eikonal approximation the problem of MHD stability of large m-number modes can be reduced to solving a single ordinary differential equation on each field line.[1] This type of large-m approximation has also been used for studying the effect of finite Larmor radius on ballooning modes in nonaxisymmetric tandem mirrors.[2-4] In one of these calculations[4] the finite Larmor radius effects stabilized all large m modes down to the limit of validity of the eikonal approximation for typical tandem mirror parameters. The largest value of ρ_i/R_p for an originally stable mode was found to be an order of magnitude smaller than present day experiments.

Because of the large stabilizing effect that finite Larmor radius corrections have on large m modes, it has been hypothesized that perhaps the most unstable MHD mode is the m = 1 "rigid" perturbation.[5] A rigid mode is characterized by a perturbation, $\vec{\xi}$, that is a function only of the distance along the magnetic field. Finite Larmor radius corrections have no effect on the

MHD stability of a rigid perturbation since the perpendicular $\underline{E}$ field is constant and ions and electrons see the same perturbation irrespective of their orbits. It was found[5] that the rigid perturbation gave more pessimistic stability criteria than the simple interchange mode but better than infinite-m MHD. With a rigid mode the vacuum contribution to the perturbed potential energy becomes important. In the limit where a boundary of the conducting wall coincides with the plasma boundary the rigid mode becomes flute-like and the beta limit is the same as the interchange beta limit.

We consider the low mode number MHD stability, with finite Larmor radius corrections, of a plasma in a simple tandem mirror. By low mode number we mean in the range of 1 to 12. Our calculations pertain primarily to the Phaedrus tandem mirror experiment. Our stability analysis is based on a formalism developed by Newcomb[6-8] which considers the equilibrium and stability of collisionless systems in the paraxial or long, thin limit. Included are rotational effects due to an ambipolar potential and finite Larmor radius effects.

Here, we consider linear modes. A variational principle is constructed using the linearized equations of motion derived from Newcomb's Lagrangian. This variational principle is solved by expanding the normal modes in terms of a 3-D set of basic functions and solving for the coefficients by a Rayleigh-Ritz method. Using this method the effect of the quadrupole nature of the equilibrium on the normal modes is represented and the possibility of poloidal and radial mode components coupling due to the non-axisymmetric geometry is taken into account.

II. Equilibrium

We will use the magnetic flux coordinates (ψ,θ,ℓ) where $\vec{B} = \vec{\nabla}\psi \times \vec{\nabla}\theta$. Here, ψ is the flux coordinate, θ is an angle-like coordinate and ℓ is the distance along a field line. The pressure components are assumed independent of θ so that at a particular axial location the constant ψ surfaces are also constant pressure surfaces.

The equilibrium is assumed to satisfy the tensor pressure magnetostatic equations[9,10]

$$\vec{j} \times \vec{B} = \nabla \cdot \vec{\vec{P}} \ , \tag{1a}$$

$$\nabla \times \vec{B} = \mu_0 \vec{j} \ , \tag{1b}$$

$$\nabla \cdot \vec{B} = 0 \ , \tag{1c}$$

where $\vec{\vec{P}} = p_\perp \vec{\vec{I}} + (p_\parallel - p_\perp)\hat{b}\hat{b}$. Here, $\hat{b}$ is a unit vector in the direction of the magnetic field $\vec{B}$ and $p_\perp$ and $p_\parallel$ are the pressure components perpendicular and parallel to $\vec{B}$, respectively.

To avoid complexity we will assume very low beta so that the equilibrium magnetic field can be taken to be the vacuum magnetic field. This is consistent with beta values attainable in Phaedrus ($\lesssim 5\%$). Also, assuming a large-aspect-ratio system, $\lambda = L_\perp/L_\parallel << 1$, to lowest order in λ^2 we have

$$d\ell = dz \ (1 + O(\lambda^2)) \ , \tag{2a}$$

$$\vec{B} \cdot \vec{z} = |B| \ , \tag{2b}$$

where B is the magnitude of the magnetic field. Using the long, thin approximation the coordinates ψ,θ are given by

$$\psi = \frac{1}{2} B(z)\left[e^{-2c(z)}\ x^2 + e^{2c(z)}\ y^2\right] , \tag{3a}$$

$$\theta = \tan^{-1}\left[\frac{y}{x}\ e^{2c(z)}\right] . \tag{3b}$$

$B(z)$ is the magnitude of the magnetic field on axis and $e^{2c(z)}$ is the ellipticity of a magnetic flux surface. The metric tensor elements for this coordinate system are,

$$(\nabla\psi)^2 = 2\psi B(z)\left[\cosh 2c(z) - \sinh 2c(z)\cos 2\theta\right] , \tag{4a}$$

$$(\nabla\theta)^2 = \frac{1}{2\psi} B(z)\left[\cosh 2c(z) + \sinh 2c(z)\cos 2\theta\right] , \tag{4b}$$

$$\nabla\theta \cdot \nabla\psi = B(z)\sinh 2c(z)\sin 2\theta . \tag{4c}$$

Also $\nabla\ell \cdot \nabla\ell = 1$ and the remaining metric tensor elements are zero. Note that $\nabla\psi$ and $\nabla\theta$ are not orthogonal. We will adopt pressure profiles based on experimental observations. The partial pressures will each be assumed separable

$$\frac{\partial}{\partial\psi}\left(\frac{p_{\parallel i} + p_{\perp i}}{2}\right) = \frac{\partial\overline{p}_i}{\partial\psi}\, g_i(\ell) , \tag{5}$$

where the function $g_i(\ell)$ depends only on the axial location and $\overline{p}_i = \overline{p}_i(\psi)$, is a function of ψ only.

The components of the curvature to lowest order in the long, thin approximation are given by

$$\vec{\kappa} = x''\hat{x} + y''\hat{y} \ , \tag{6}$$

where the prime indicates the derivative with respect to z. The covariant components of the curvature in the (ψ,θ,ℓ) coordinate system can be written as

$$\kappa_\psi = \kappa_0 + \kappa_1 \cos 2\theta \ , \tag{7a}$$

$$\kappa_\beta = -2\psi\kappa_1 \sin 2\theta \ , \tag{7b}$$

where $\kappa_0 = \frac{1}{2}(\sigma\sigma'' + \tau\tau'')$, $\kappa_1 = \frac{1}{2}(\sigma\sigma'' - \tau\tau'')$,

with $\sigma(z) \equiv \sqrt{\frac{1}{B(z)}}\, e^{c(z)}$, $\tau(z) \equiv \sqrt{\frac{1}{B(z)}}\, e^{-c(z)}$.

In a quadrupole tandem mirror there is also a parallel current due to the non-axisymmetric nature of the equilibrium. Using Eqs. (1) and assuming the current vanishes at each end of the device the parallel current is given by

$$\frac{j_\parallel}{B}\left(1 + \frac{p_\perp - p_\parallel}{B^2}\right) = \int_{z_0}^{z} dz\, \frac{\kappa_\theta}{B}\frac{\partial}{\partial\psi}(p_\perp + p_\parallel) \ . \tag{8}$$

The low beta, long, thin equilibrium used for the stability analysis presented below is described by the functions B(z), C(z), the axial pressure distributions, $g_i(\ell)$, $g_e(\ell)$ and the radial pressure distributions $\overline{p}_i(\psi)$, $\overline{p}_e(\psi)$. The functions B(z) and C(z) for the Phaedrus tandem mirror are shown in Figs. 1a

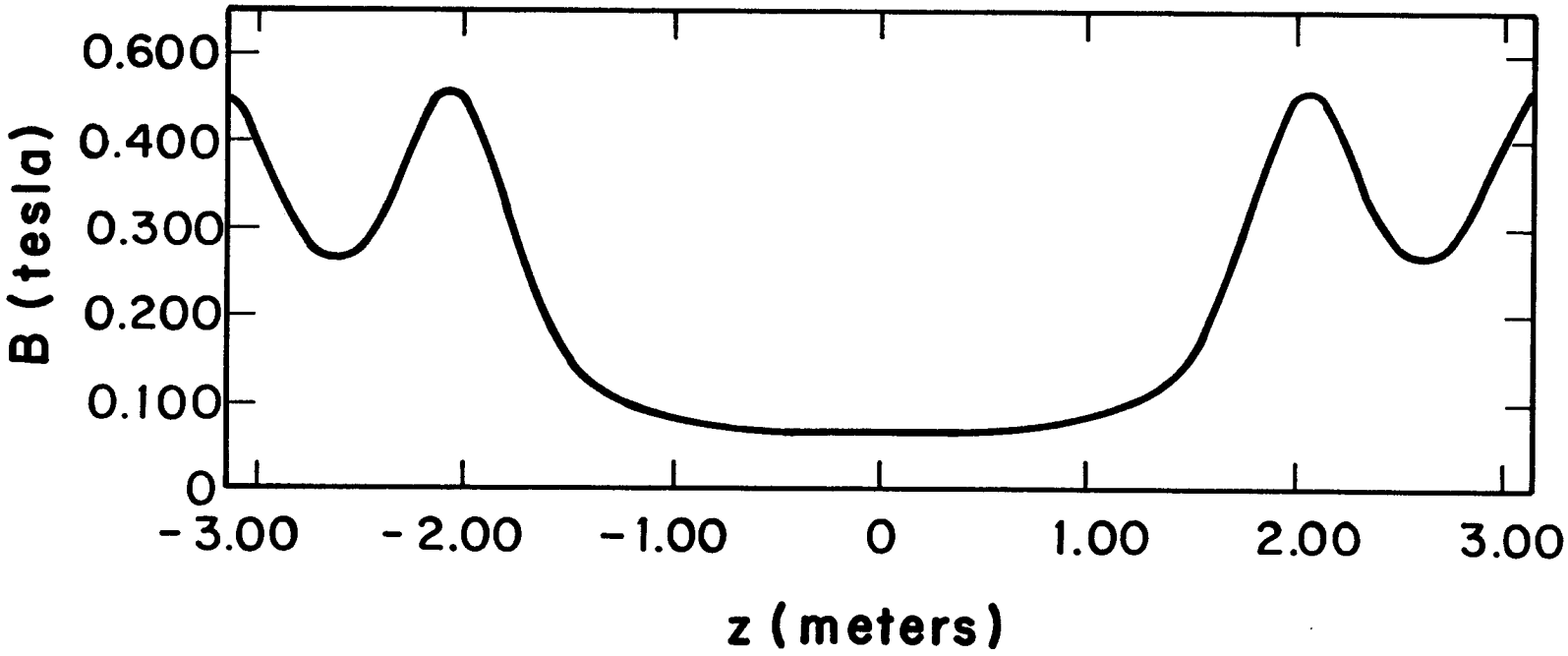

Fig. 1(a). Axial variation of the magnetic field, B(z), in the Phaedrus tandem mirror.

and 1b, respectively. These functions were calculated using field line data from the EFF1 code[11] using the Phaedrus coil set as input. The model axial pressure distribution, $g_i(\ell)$, used here is shown in Fig. 2. The radial pressure distribution used is

$$p_i(\psi) = p_o \cos^2 \left(\frac{\pi}{2}\sqrt{\frac{\psi}{\psi_e}}\right)$$

where p_o is the pressure on axis and ψ_e is the flux surface on the edge of the plasma.

III. Stability

The stability analysis we use is based on the Lagrangian analysis developed by Newcomb[6-8] for equilibrium and stability of collisionless systems including finite Larmor orbit corrections in the paraxial limit. We apply this analysis to the problem of linear stability in a long, thin quadrupole tandem mirror. In the derivation of Newcomb's equations two expansion parameters were used, the ratio of gyroradius to radial scale length and the ratio of radial to axial scale length λ.

The Lagrangian density is

$$L = \frac{1}{2}\left(\rho\vec{x}_t^2 + S\vec{x}_t \cdot \vec{x}_\theta - R\vec{x}_\theta^2 - Q\vec{x}_z^2\right), \tag{9}$$

where $\vec{x}(\psi,\theta,z,t)$ is a two component vector (x,y) giving the position of a magnetic field line. The subscripts indicate partial derivatives. Also,

$$Q = B^2 + p_\perp - p_\parallel, \tag{10}$$

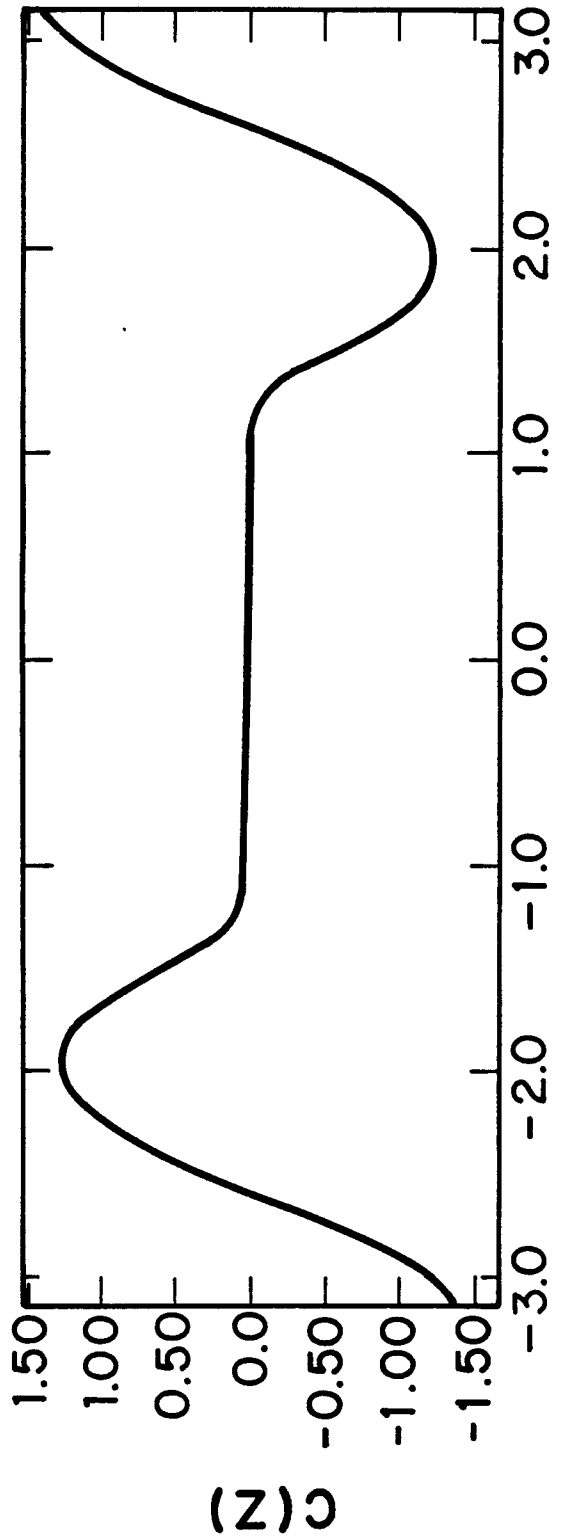

Fig. 1(b). The function C(z), where exp 2C(z) is the ellipticity of a magnetic flux surface.

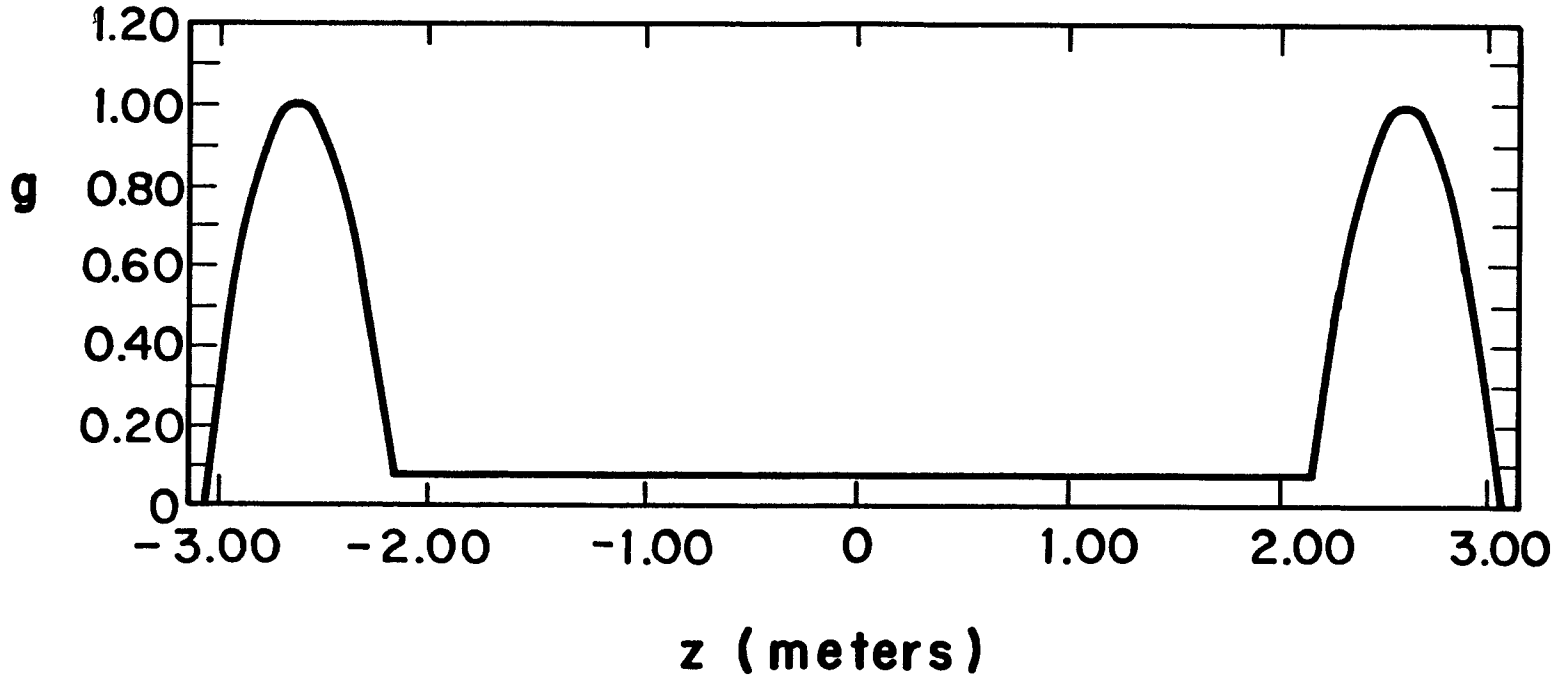

Fig. 2. Model axial pressure distribution for the Phaedrus tandem mirror: $\frac{\partial \overline{p}}{\partial \psi} = g(\ell)\, \frac{1}{2}\, \frac{\partial}{\partial \psi}\, (p_{\perp} + p_{||})$.

$$S = 2\rho\Phi_\psi - \frac{1}{2}\frac{1}{B}(MB^2)_\psi \ , \tag{11}$$

$$R = -\rho\Phi_\psi^2 + \frac{1}{2B}(MB^2)_\psi\Phi_\psi - \frac{1}{B}K_\psi B_\psi \ , \tag{12}$$

$$M = -8\pi B \sum \frac{m^2}{e} \int f\nu \frac{d\nu d\varepsilon}{q} \ , \tag{13}$$

$$K = 2\pi B^3 \sum \frac{m^3}{e^2} \int f\nu^2 \frac{d\nu d\varepsilon}{q} \ , \tag{14}$$

where ρ is the mass density, Φ is the equilibrium ambipolar potential and f is the distribution function and is a function of ψ, ν, ε. Here, ν is the magnetic moment per unit mass, ε is the energy per unit mass and q is the parallel velocity. All equilibrium quantities are functions only of ψ and z.

The equations of motion are obtained from Hamilton's principle, $\delta \int L \frac{d\psi d\theta dz}{B} = 0$ together with the incompressibility constraint condition $(x_\psi y_\theta - x_\theta y_\psi) = 1/B$, to yield

$$\vec{F} = \rho\vec{x}_{tt} - B(Q\vec{x}_z/B)_z + S\vec{x}_{\theta t} - R\vec{x}_{\theta\theta} = 0 \ . \tag{15}$$

Linearizing the variable $\vec{x}$, in the form $\vec{x} = \vec{x}^{(o)} + \vec{\xi}$ we obtain the following linearized equations of motion

$$\vec{\xi}_\psi \cdot \vec{F}^{(o)} + \vec{x}_\psi^{(o)} \cdot \delta\vec{F} = 0 \ , \tag{16a}$$

$$\vec{\xi}_\theta \cdot \vec{F}^{(o)} + \vec{x}_\theta^{(o)} \cdot \delta\vec{F} = 0 \ , \tag{16b}$$

where $$\vec{F}^{(o)} = -B\left(\frac{Q}{B}\vec{x}_z^{(o)}\right)_z - R\vec{x}_{\theta\theta}^{(o)}$$

and $\delta\vec{F}$ is the same as Eq. (15) except with $\vec{\xi}$ substituted for $\vec{x}$. Writing $\vec{\xi}$ in terms of contravariant components $\vec{\xi} = X\vec{x}_\psi + Y\vec{x}_\theta$ where $X = \vec{\xi} \cdot \nabla\psi$ and $Y = \vec{\xi} \cdot \nabla\theta$, the linearized incompressibility condition is given by

$$\left(\frac{X}{B}\right)_\psi + \frac{Y_\theta}{B} = 0 \ . \tag{17}$$

To obtain a variational principle we multiply Eq. (16a) by X^* and integrate over volume, multiply Eq. (16b) by Y^* and integrate over volume, and then sum the two to obtain

$$\frac{1}{2}\int \frac{d\psi d\theta dz}{B}\{\rho\vec{\xi}^* \cdot \vec{\xi}_{tt} + S\vec{\xi}^* \cdot \vec{\xi}_{\theta t} - R\vec{\xi}^* \cdot \vec{\xi}_{\theta\theta} - R(X^*\vec{\xi}_\psi \cdot \vec{x}^{(o)}_{\theta\theta} + Y^*\vec{\xi}_\theta \cdot \vec{x}^{(o)}_{\theta\theta})\} + W(\vec{\xi}^*,\vec{\xi}) = 0 \ , \tag{18}$$

where

$$W(\vec{\xi}^*,\vec{\xi}) = \frac{1}{2}\int \frac{d\psi d\theta dz}{B}\left\{\frac{Q}{B^2}\left[\nabla\theta \cdot \nabla\theta X_z^2 - \nabla\theta \cdot \nabla\psi(X_z^* Y_z + X_z Y_z^*) + \nabla\psi \cdot \nabla\psi Y_z^2\right] - (p_\perp + p_\parallel)_\psi \kappa_\psi X^2 + Q\frac{j_\parallel}{B^2}(X^* Y_z + X Y_z^*)\right\} \ . \tag{19}$$

The function $W(\vec{\xi}^*,\vec{\xi})$ is Newcomb's ideal MHD energy integral in the paraxial approximation.[8]

We will defer treatment of rotational modes to a future paper and here will take $R = 0$. Equation (17) suggests X and Y can be written in terms of a stream function. Since $B^{-1}B_\psi$ is $O(\lambda^2)$, X and Y can be given to $O(\lambda^2)$ by

$$X = \phi_\theta \tag{20a}$$

$$Y = -\phi_\psi \ . \tag{20b}$$

It is assumed $\vec{\xi} \propto \exp(i\omega t)$. Substituting $\vec{\xi} = B^{-1}\hat{b}x[\phi_\theta \nabla\theta + \phi_\psi \nabla\psi] \exp(i\omega t)$ into Eq. (18) and dropping terms with R gives the following variational princple expressed in terms of ϕ,

$$\omega^2 K(\phi^*,\phi) + \omega F(\phi^*,\phi) + W(\phi^*,\phi) = 0 \ , \tag{21}$$

where
$$K(\phi^*,\phi) = -\frac{1}{2}\int \frac{d\psi d\theta dz}{B^3} \rho[\nabla\theta\phi_\theta + \nabla\psi\phi_\psi]^2 \ , \tag{22a}$$

$$F(\phi^*,\phi) = \frac{i}{2}\int \frac{d\psi d\theta dz}{B^3} S[\nabla\theta\phi^*_\theta + \nabla\psi\phi^*_\psi] \cdot \frac{\partial}{\partial\theta}[\nabla\theta\phi_\theta + \nabla\psi\phi_\psi] \ , \tag{22b}$$

$$W(\phi^*,\phi) = \frac{1}{2}\int \frac{d\psi d\theta dz}{B} \{\frac{Q}{B^2}[\nabla\theta\phi_{\theta z} + \nabla\theta\phi_{\psi z}]^2$$

$$- (p_\perp + p_\parallel)_\psi \kappa_\psi \phi_\theta^2 - \frac{Qj_\parallel}{B^2}(\phi^*_\theta\phi_{z\psi} + \phi_\theta\phi^*_{z\psi})\} \ . \tag{22c}$$

Equation (21) with Eqs. (22) will be used for calculating the normal modes of the system.

IV. Numerical Method of Solution

Equation (21) is solved for the normal modes of the system by a Rayleigh-Ritz method. The stream function ϕ is expanded in terms of a finite set of basis functions,

$$\phi(\psi,\theta,z) = \sum_k \sum_n \sum_{\substack{m \\ m\neq 0}} \phi_{knm} U_k(z) V_n(\psi) e^{im\theta} = \sum_k \sum_n \sum_{\substack{m \\ m\neq 0}} a_{knm} \phi_{knm} \tag{23}$$

where $\phi_{knm} = U_k(z)\ V_n(\psi)\ e^{im\theta}$. For $U_k(z)$ we use a Fourier series and for $V_n(\psi)$ we use Bessel functions of order 2. In Phaedrus to adequately represent the modes 40 (20 odd and 20 even) $U_\kappa(z)$ functions were needed and 10 $V_n(\psi)$ functions. The number 40 for the number of axial basis functions was arrived at by comparing two different techniques for solving the infinite n ballooning mode equation. The first technique was a shooting method and the second technique involved expanding the solution in terms of axial basis functions. It was found that 40 axial basis functions gave very good agreement between the two methods.

The boundary conditions on the function ϕ are that ϕ must go to zero at the surface of the conducting wall surrounding the plasma in order to have $\vec{\xi} \cdot \hat{n} = 0$, where $\hat{n}$ is the normal to the conducting surface. Also, ϕ must go to zero at $r = 0$ for $\vec{\xi}$ to be finite. The problem of finding the normal modes is thus reduced to finding the solution of the matrix problem

$$\vec{\vec{W}}\vec{a} = -\omega^2\vec{\vec{K}}\vec{a} - \omega\vec{\vec{F}}\vec{a} \ , \tag{24}$$

where the vectors $\vec{a}$ are composed of elements a_{knm} and the matrix $\vec{\vec{W}}$ is composed of elements $\vec{\vec{W}}_{k'n'm'\kappa nm} = W(\phi^*_{k'n'm'}, \phi_{\kappa nm})$, etc. The matrix elements are real and $\vec{\vec{W}}$, $\vec{\vec{K}}$ and $\vec{\vec{F}}$ are symmetric matrices.

Since the quadrupole nature of the magnetic field has been included, each m component of ϕ will couple to the m ± 2 components. Also, if the m component is symmetric with respect to reflection about z = 0, then it couples to the antisymmetric parts of the m ± 2 components. Hence, one can solve separately for even and odd m modes and there will be two types of even modes:

one when the m = 2 component has even symmetry with respect to reflection about z = 0 and another where the m = 2 component is antisymmetric.

Equation (24) is solved on the computer using a mathematical subroutine which solves the general problem $\vec{\vec{A}}\vec{x} = \lambda\vec{\vec{B}}\vec{x}$ for the eigenvectors $\vec{x}$ and eigenvalues λ where $\vec{\vec{A}}$ and $\vec{\vec{B}}$ are real square matrices. Equation (24) can be put into this form by defining another vector, $\vec{v}$, such that $\vec{v} = \omega\vec{a}$. Equation (24) can then be written as

$$\begin{pmatrix} \vec{\vec{W}} & 0 \\ 0 & -\vec{\vec{K}} \end{pmatrix}\begin{pmatrix} \vec{a} \\ \vec{v} \end{pmatrix} = \omega \begin{pmatrix} -\vec{\vec{F}} & -\vec{\vec{K}} \\ -\vec{\vec{K}} & 0 \end{pmatrix}\begin{pmatrix} \vec{a} \\ \vec{v} \end{pmatrix} . \tag{25}$$

In this equation the matrices are also symmetric but the right-hand matrix is not positive definite and hence the eigenvalues, ω, can be complex.

Outside the main plasma column we allow for an exterior region containing pressureless plasma. In the limit where the density in this region goes to zero one obtains the same answer for the most unstable mode as one would get if this region were filled with a vacuum.[5] When the exterior region is allowed to have a small amount of density there is a stabilizing effect due to the extra inertia provided by the plasma in this region. This has the effect of reducing the growth rate somewhat over what one would get if this region were filled with vacuum. For ideal MHD the marginally stable point is still the same. However, when FLR effects are included, the region of stability is increased.

V. Results

In Fig. 3 the MHD beta limits with no finite Larmor radius effects are given for the Phaedrus configuration. Instability occurs when the bad curvature weighting central cell pressure, here measured by $\beta_{cc} \equiv$ central cell per-

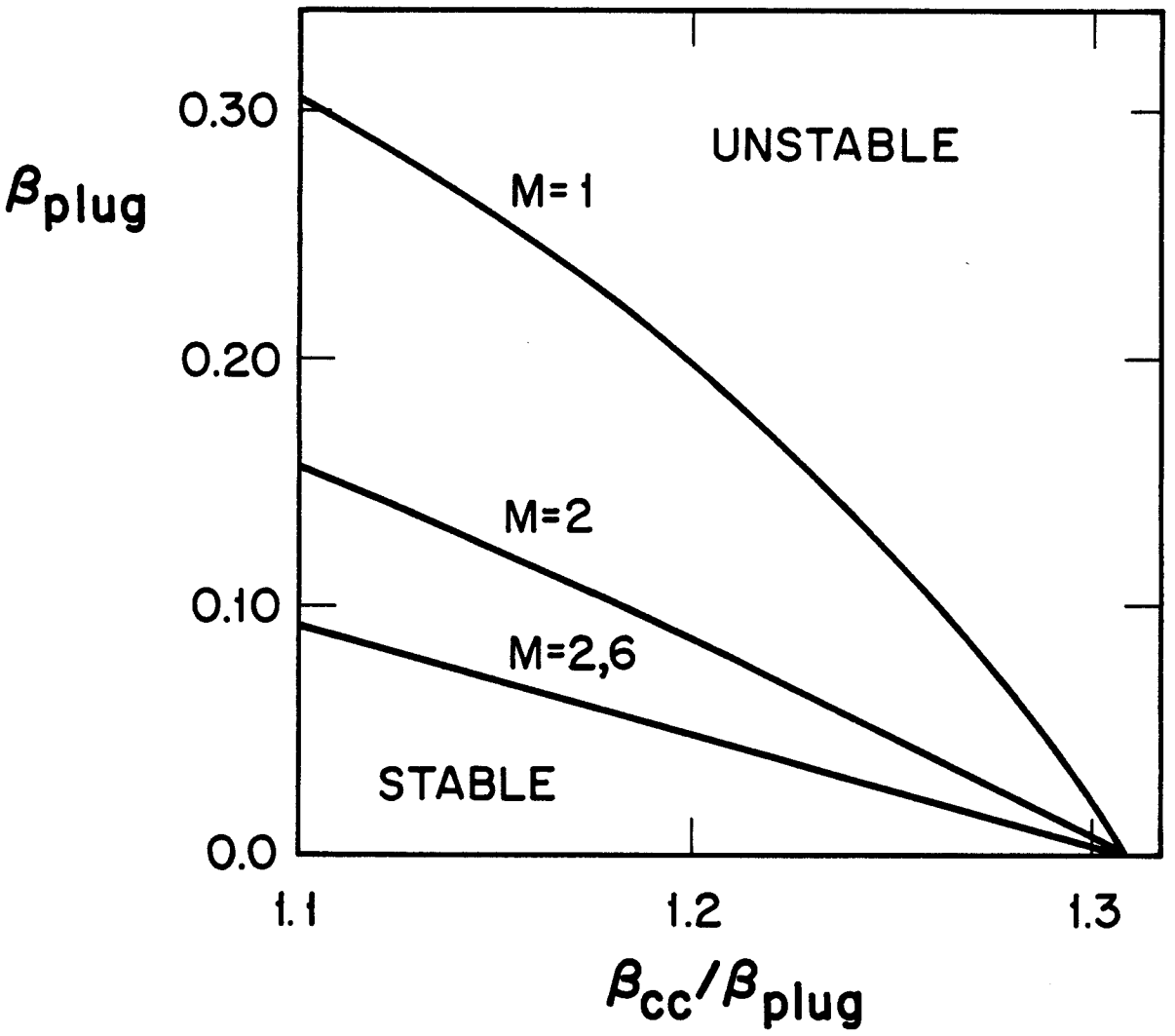

Fig. 3. Ideal MHD beta limits for the Phaedrus tandem mirror. The values of m indicate the dominant poloidal mode component.

pendicular plasma pressure/magnetic field pressure, becomes too large relative to the good curvature weighting end plug pressure indicated by β_{plug}, which is measured at the plug midplane. The abscissa β_{plug}/β_{cc} is a measure of the average radial magnetic well depth in the tandem mirror. Figure 3 illustrates the tendency in pure MHD for higher m modes to be more unstable than lower m modes. Also, for the ideal MHD case there is a large amount of coupling between the different m modes, particularly as m is increased. The modes were composed mainly of components with even symmetry and were for the most part interchange-like with some ballooning in the bad curvature region at higher values of β.

When finite Larmor radius effects are included the most unstable modes tended to become more and more composed of a single low m number as ρ_i/R_p was increased. This is illustrated in Fig. 4 for the case of marginally stable even modes at fixed β_{cc}/β_{plug}. For $\rho_i/R_p = 0$ the mode was composed of almost equal parts m = 2 and m = 6 with some m = 10. When $\rho_i/R_p > 0.02$ in the plug, the m = 2 component comprises 94% of the mode. When finite Larmor radius effects are included the m = 2 is the most unstable even mode, but even it is stabilized for $\rho_i/R_p > 0.05$.

The large stabilizing effect of finite Larmor radius corrections is further demonstrated in Fig. 5. Here, the growth rate of various odd modes is plotted for increasing ρ_i/R_p in the plug. The beta ratio β_{cc}/β_{plug} exceeds the interchange limit. Here, the ratio of control cell to plug beta was kept fixed while the ion gyroradius was varied. For $\rho_i/R_p = 0$ the growth rates were higher for higher m number modes. However, as ρ_i/R_p increases the higher m modes quickly stabilize and for $\rho_i/R_p > 0.04$ only the m = 1 mode is un-

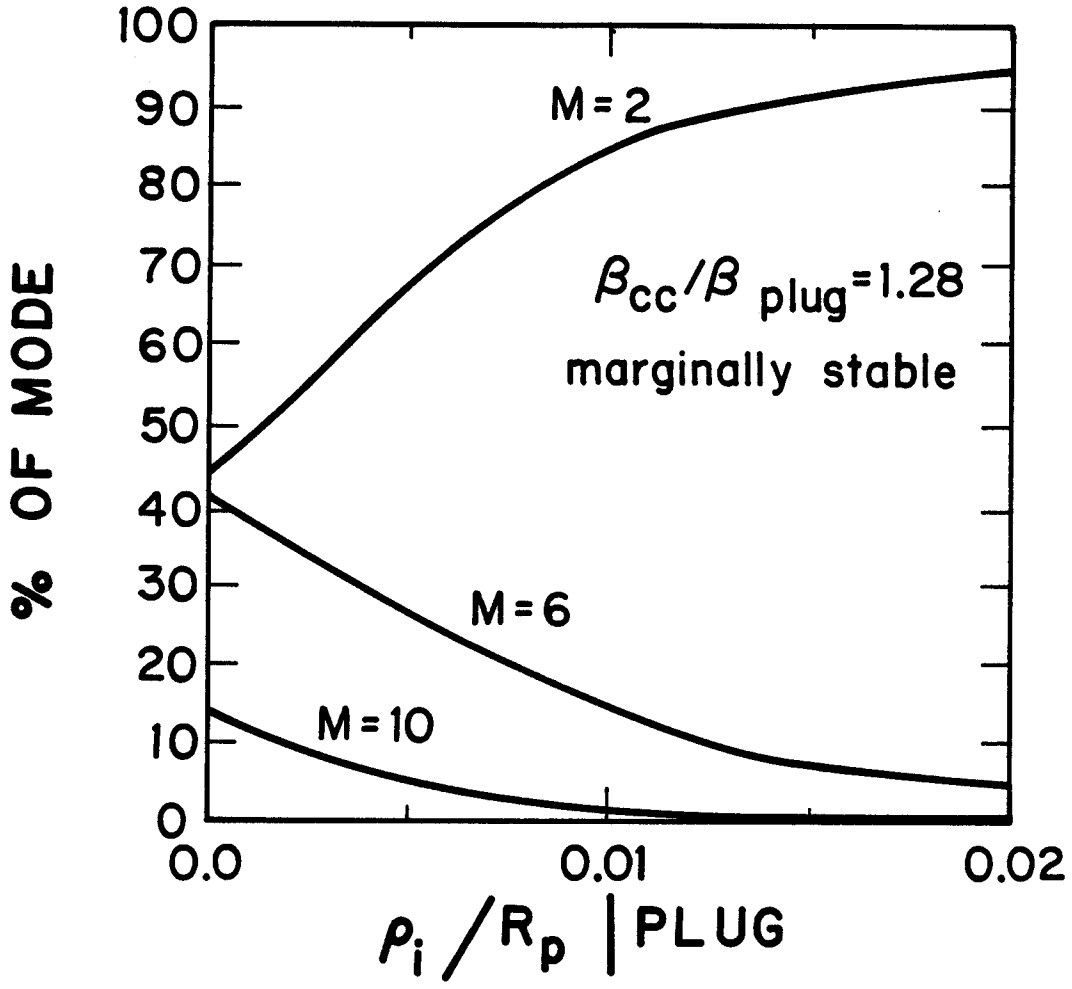

Fig. 4. Spectral components of marginally stable even poloidal mode number modes, for $\beta_{cc}/\beta_{plug} = 1.28$. The ratio β_{cc}/β_{plug} is fixed and β is changed to keep the mode marginally stable as ρ_i/R_p is increased.

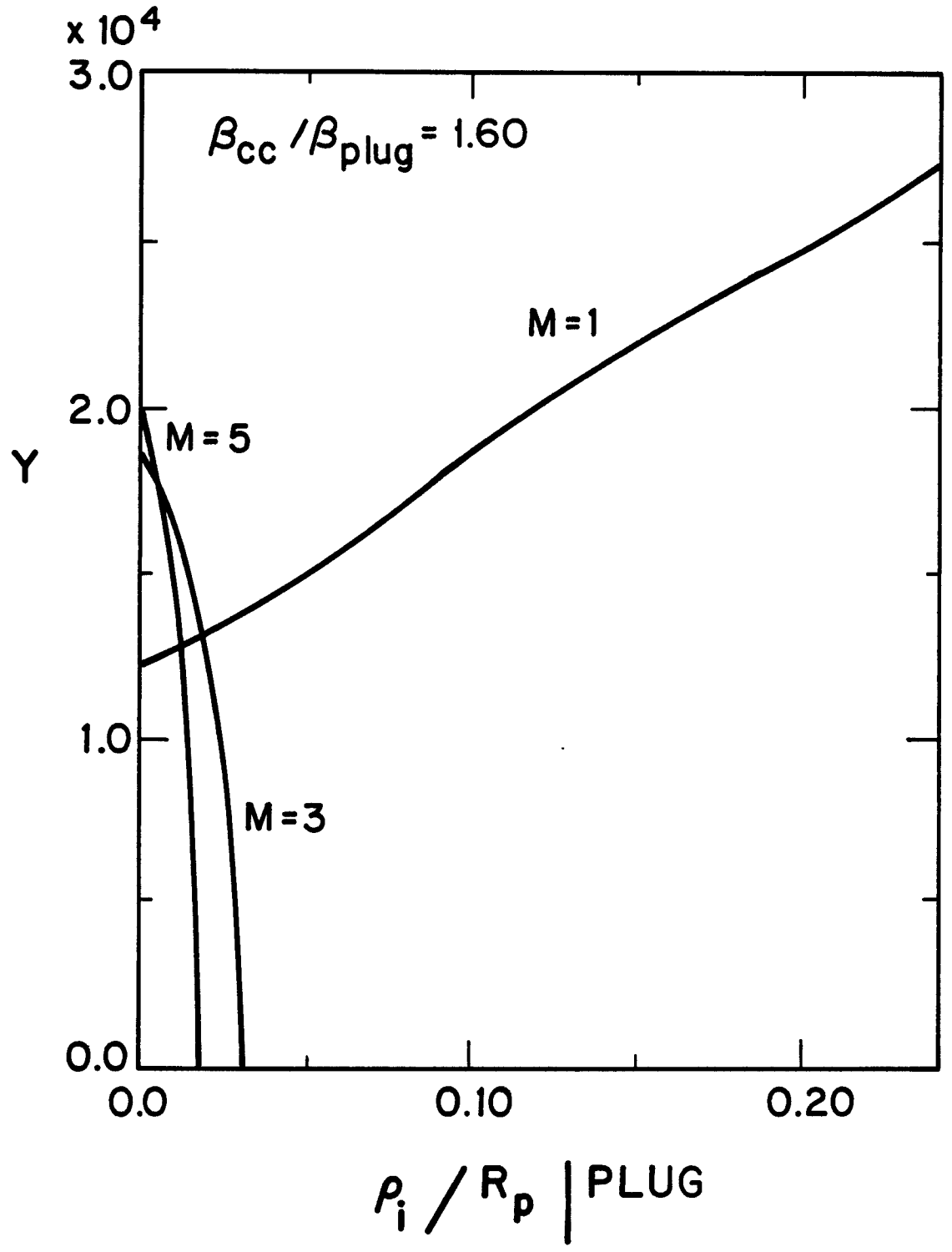

Fig. 5. Growth rate of odd poloidal mode number modes in Phaedrus for fixed $\beta_{cc}/\beta_{plug} = 1.60$, varying ρ_i.

stable. In Phaedrus $\rho_i/R_p \approx 0.02$ so one would expect to see only the m = 1 mode based on these results.

Figures 6a and 6b show the change in the mode structure of the m = 1 mode as ρ_i/R_p increases. The m = 1 mode becomes a rigid displacement when ρ_i/R_p increases because this type of perturbation minimizes the effect of the finite Larmor radius terms. The next most unstable mode would be expected to be the m = 2 mode. The m = 2 mode is stable for Phaedrus parameters but for small ρ_i/R_p the stream function inside the plasma is proportional to r as in the case of the m = 1 perturbation. This type of perturbation seems to minimize the stabilizing effect of FLR even for $m \neq 1$.

In summary, we have studied the full 3-D MHD with finite Larmor radius effects stability in the Phaedrus tandem mirror. The most unstable mode was found to be an m = 1 rigid perturbation which, because of the low beta, was essentially interchange-like. A mode satisfying this description has been observed in Phaedrus.[12]

In our calculations the m = 1 mode was "pure" with almost no coupling to adjacent m components for Phaedrus parameters. However, the coupling between the m components is proportional to the amount of axial variation of the mode. Hence, the "pure" nature of the mode may be a consequence of the low beta.

In a longer, higher beta tandem mirror where the rigid mode has more axial variation the coupling of the various m components due to the nonaxisymmetric geometry may be larger. This is currently being investigated.

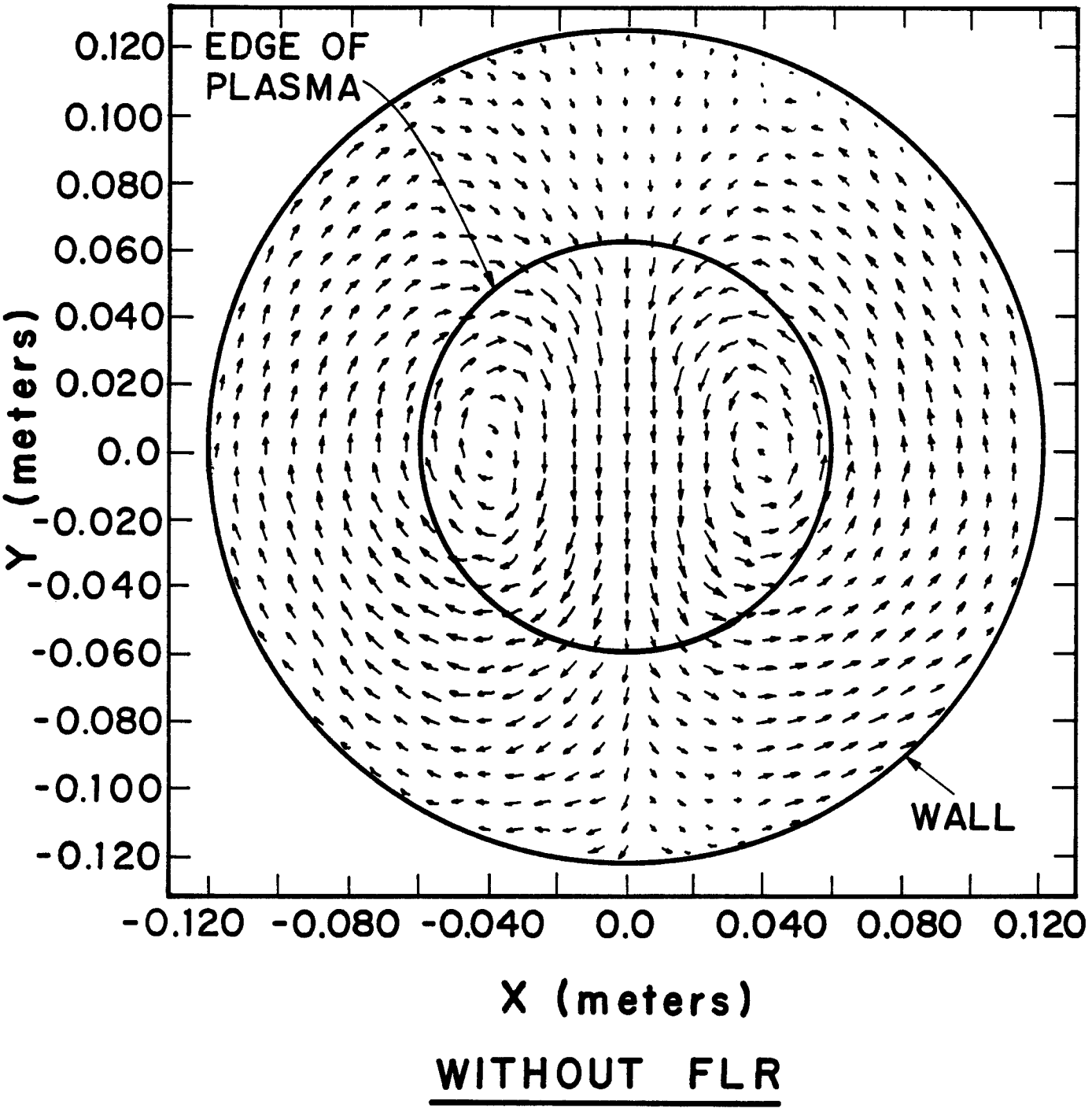

Fig. 6(a). Displacement vector, $\vec{\xi}$, for the m = 1 mode without FLR effects.

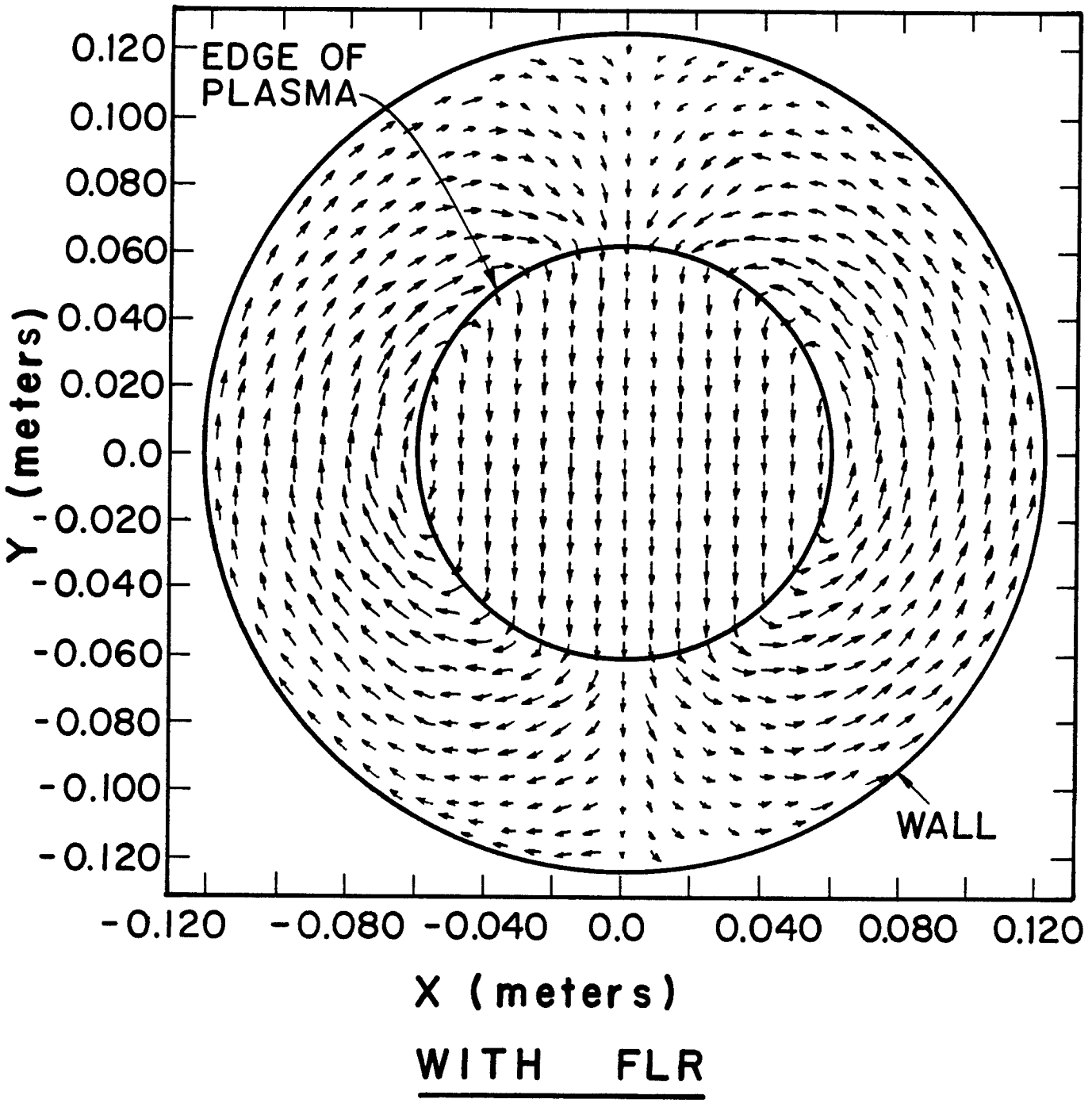

Fig. 6(b). Displacement vector, $\vec{\xi}$, for the m = 1 mode with ($\rho_i/R_p > 0.04$) FLR effects.

Acknowledgment

The authors would like to thank R.A. Breun and N. Hershkowitz for their interest and help in this work and would also like to acknowledge useful discussions with T.B. Kaiser and W.M. Nevins. This work was supported by the U.S. Department of Energy under contract no. DE-AC02-80ER53104.

References

1. T.B. Kaiser and L.D. Pearlstein, Lawrence Livermore National Laboratory, May 10, 1982, UCRL-87659 preprint.

2. W.M. Tang and P.J. Catto, Phys. Fluids 24, 1314 (1981).

3. X.S. Lee and P.J. Catto, Phys. Fluids 24, 2010 (1981).

4. R.H. Bulmer, T.B. Kaiser, W.M. Nevins, W.A. Newcomb, L.D. Pearlstein, H.R. Strauss, S. Wollman and M. Wakatami, Plasma Phys. and Controlled Nuclear Fusion Research 1982, (IAEA, Baltimore, 1983), Vol. I, p. 531.

5. T.B. Kaiser, W.M. Nevins and L.D. Pearlstein, Phys. Fluids 26, 351 (1983).

6. W.A. Newcomb, Ann. Phys. 81, 231 (1973).

7. W.A. Newcomb, Mirror Theory Monthly, Lawrence Livermore National Laboratory (Sept. 15, 1981).

8. W.A. Newcomb, J. Plasma Phys. 26, 529 (1981).

9. L.S. Hall and B. McNamara, Phys. Fluids 18, 552 (1975).

10. L.D. Pearlstein, T.B. Kaiser and W.A. Newcomb, Phys. Fluids 24, 1326 (1981).

11. S.J. Sachett, LLNL Report UCRL-52402 (1978).

12. A.W. Molvik, R.A. Breun, S.N. Golovato, N. Hershkowitz, B. McVey, D. Smatlak, and L. Yujiri, Phys. Rev. Lett. 48, 742 (1982).